Optical Coherence Tomography for Neurosurgical Imaging of Human Intracortical Melanoma

Stephen A. Boppart, Ph.D.,
Mark E. Brezinski, M.D., Ph.D., Costas Pitris, M.S.E.E.,
James G. Fujimoto, Ph.D.

Department of Electrical Engineering and Computer Science (SAB, CP, JGF), Research Laboratory of Electronics, Massachusetts Institute of Technology, Cambridge, Harvard-MIT Division of Health Sciences and Technology (SAB, CP), Massachusetts Institute of Technology, Cambridge, and Cardiac Unit (MEB), Massachusetts General Hospital and Harvard Medical School, Boston, Massachusetts

OBJECTIVE: Intraoperative identification of brain tumors and tumor margins has been limited by either the resolution of the in vivo imaging technique or the time required to obtain histological specimens. Our objective was to evaluate the feasibility of using optical coherence tomography (OCT) as a high-resolution, real-time intraoperative imaging technique to identify an intracortical melanoma.

INSTRUMENTATION: OCT is a new, noncontact, high-speed imaging technology capable of resolutions on the micrometer scale. OCT is analogous to ultrasound B-mode imaging, except that reflections of infrared light, rather than sound, are detected. OCT uses inherent tissue contrast, rather than enhancement with dyes, to differentiate tissue types. The compact, fiberoptic-based design is readily integrated with surgical instruments.

METHODS: A portable handheld OCT surgical imaging probe has been constructed for imaging within the surgical field. Cadaveric human cortex with metastatic melanoma was harvested and imaged in two and three dimensions. Changes in optical backscatter intensity were used to identify regions of tumor and to locate tumor margins. Structures within the optical coherence tomographic images were compared with the histological slides.

RESULTS: Two-dimensional images showed increased optical backscatter from regions of tumor, which was quantitatively used to determine the tumor margin. The images correlated well with the histological findings. Three-dimensional reconstructions revealed regions of tumor penetrating normal cortex and could be resectioned at arbitrary planes. Subsurface cerebral vascular structures could be identified and were therefore avoided.

CONCLUSION: OCT can effectively differentiate normal cortex from intracortical melanoma based on variations in optical backscatter. The high-resolution, high-speed imaging capabilities of OCT may permit the intraoperative identification of tumor and the more precise localization of tumor margins. (Neurosurgery 43:834–841, 1998)

Key words: Imaging, Infrared, Margins, Microscopy, Optical, Stereotactic, Tumor

Imaging modalities, including ultrasonography, computed tomography, and magnetic resonance imaging, have been used to locate central nervous system tumors and identify tumor margins (1, 7, 10, 12, 24, 25). Unfortunately, the resolutions of such modalities are often hundreds of micrometers, thereby poorly resolving small tumors and reducing the sharp definition of the tumor margin. Furthermore, the registration of images with tissue at the submillimeter level is problematic and ongoing research is being conducted to explore means of stereotactically aligning the two (13). Optical techniques, including fluorescence and Raman spectroscopy, have enabled quantitative identification of brain tumor cells and tumor margins based on detected spectra (14, 15, 18, 20, 21). However, image representation of tumors based on these techniques is limited to surface features without cross-sectional imaging or optical ranging into the tissue. A technology capable of performing intraoperative cross-sectional imaging of tissue at near-histological resolutions could provide high-resolution discrimination between normal and pathological tissue. If this high-resolution cross-sectional imaging could be

performed in real time, it would be a powerful tool for the surgeon resecting central nervous system neoplasms, allowing tumor margins to be rapidly defined intraoperatively.

Optical coherence tomography (OCT) is a new high-speed, micrometer-resolution imaging modality based on the detection of backscattered infrared light (17). Because OCT relies on inherent variations in the tissue index of refraction and optical scattering, no exogenous intravenously administered or topically applied dyes are necessary to enhance contrast between normal and pathological tissue. OCT was first used to image the transparent structures of the human eye and has been clinically applied in ophthalmology for the diagnosis and management of retinal disease (16, 22). More recently, the use of longer wavelengths, which are absorbed and scattered less in biological tissue, has permitted imaging in more highly scattering tissues, such as skin and the vascular system (6, 11, 23). As a research tool for developmental biology, OCT has been used to image the in vivo developing brain in the *Xenopus* animal model (2). The feasibility for using OCT for surgical diagnostics has been demonstrated in vitro, and in vivo catheter/endoscopic OCT of the gastrointestinal and pulmonary tracts has been demonstrated in a rabbit model (5, 28).

Several features of OCT suggest it will be useful for the guidance of surgical procedures. First, unlike magnetic resonance imaging, the OCT instrument is compact and portable, approximately the size of a personal computer. Second, unlike ultrasonography, OCT is a noncontact method, with no requirement for a transducing medium. Third, the fiber-based design allows straightforward integration with scalpels, microscopes, or pencil-sized handheld probes, which are well suited for the tight confines of the operative suite (3, 26). Fourth, OCT beam delivery instruments can be designed to perform scanning over large cortical surface areas to identify abnormalities. Suspect regions can then be imaged with high resolution over smaller areas to localize tumor margins.

In this article, we demonstrate the high-resolution two- and three-dimensional imaging capabilities that are unique to OCT and investigate the feasibility of OCT for neurosurgical imaging. An intracortical metastatic melanoma lesion was used to demonstrate high-resolution OCT. A pen-sized handheld surgical imaging probe has been constructed and was used to acquire two-dimensional cross-sectional images of cadaveric human cortex and intracortical metastatic melanoma lesions. The optical coherence tomographic images were correlated with the corresponding histological findings. Variations in optical backscatter between normal cortex and tumor were used for tumor discrimination. Three-dimensional OCT was performed on a melanoma lesion to determine the extent of tumor penetration into normal cortex. A cerebral artery was imaged and correlated with the histological findings, demonstrating the feasibility of OCT for identifying and avoiding vascular structures.

INSTRUMENTATION AND METHODS

Optical coherence tomography

OCT is a high-resolution imaging modality based on the detection of backscattered infrared light from biological tissue. The technique is somewhat analogous to ultrasound B-mode imaging, except that reflection of light, rather than sound, is detected. Because of the high velocities associated with the propagation of light, a technique known as low-coherence interferometry is used, rather than standard electronic detection methods, to determine precise ranging locations of optical backreflections from within tissue. A schematic of the OCT instrument and the beam delivery systems is shown in *Figure 1*. A superluminescent diode is used as the low-coherence light source for imaging. A low-coherence source is similar to a standard laser, except that the wavelengths of light emitted span a larger range (or bandwidth). The use of low-coherence light in an interferometer permits precise measurement of the echo time delay of backscattered light. Conceptually, low-coherence interferometry can be explained by viewing the light beam as being composed of optical pulses. An optical pulse is emitted from the source and is equally split by a fiberoptic coupler with half sent down the reference arm and half sent down the sample arm of the interferometer. The reference arm contains a me-

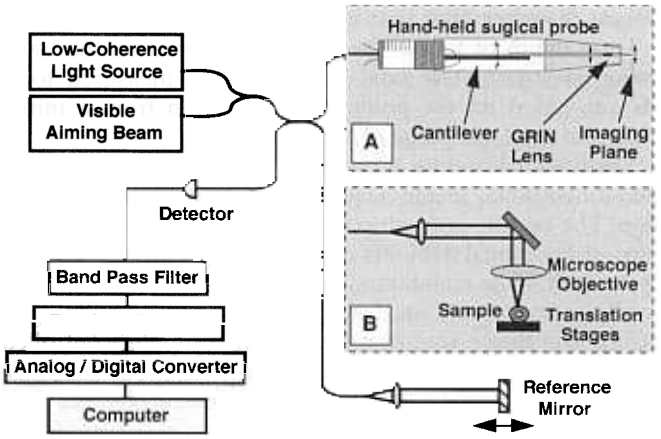

FIGURE 1. Schematic of OCT instrument and handheld surgical probe. Two sample-arm configurations for beam delivery are shown. *A*, handheld surgical imaging probe for forward-directed imaging of cortex. The compact and portable probe enables imaging within the surgical field, remote from the OCT instrument. *B*, microscope objective imaging with micrometer-precision translation stages to maintain registration for three-dimensional imaging of tissue. Reflections and optical backscatter from internal structures within the tissue are measured as the transverse position of the beam is scanned to produce two- and three-dimensional images of the tissue and pathological abnormalities.

chanical scanning reference mirror. Light in the sample arm is reflected from various depths from within the tissue. The reflections from each arm are recombined by the fiberoptic coupler, and an interference pattern is produced when the time delays of the light from the sample and the reference arms are equal. This interference is measured with a detector, demodulated, and digitized to yield a measurement of the backscattered light from within the tissue. A signal detection dynamic range of 110 dB is achieved using only 150 μW of optical power on the tissue. Each sweep of the reference arm mirror corresponds to one axial (depth) scan into the tissue. Cross-sectional images are acquired by transversely scanning the optical beam across the tissue in the plane perpendicular to the surface. Adjacent axial (depth) scans are assembled to form a two-dimensional image of backscattered light from the tissue, which is displayed in either false color or gray scale. A visible aiming beam (632 nm) is combined with the invisible infrared imaging beam (1300 nm). This permits the location of the tissue imaging plane to be visualized for later registration with the corresponding histological findings.

Two sample-arm systems (handheld probe and microscope) for beam delivery to the tissue are shown in *Figure 1*. *Figure 1A* shows a schematic of the handheld OCT surgical imaging probe used to acquire two-dimensional cross-sections of intracortical melanoma and normal cortex. This instrument is designed for forward-directed OCT and is the size of a standard ballpoint pen (3). The compact and portable nature of this handheld probe enables imaging in confined regions within the surgical field. Beam scanning is performed with a piezoelectric cantilever, which displaces a small gradient index lens. The lens focuses the 1300-nm imaging beam to a 30-μm diameter spot that is determined by measuring the 1.1-mm depth of focus. The spot size determines the transverse resolution. The axial resolution was measured to be 16 μm, based on the point spread function from a mirror placed at the focal plane of the probe.

The handheld probe is extremely compact. However, only two-dimensional image acquisition is possible with this design. The sample-arm setup in *Figure 1B* was used to acquire three-dimensional data sets of normal cortex and intracortical melanoma while maintaining precise image registration. This configuration used a fixed microscope objective and imaging beam. The tissue was translated with computer-controlled, micrometer-precision, X-Y translation stages. Three-dimensional data sets were assembled from a series of two-dimensional cross-sectional optical coherence tomographic images. The microscope objective focused the imaging beam to a 23-μm diameter spot (625-μm depth of focus) and therefore had a higher transverse resolution than the handheld probe. The 16-μm axial resolution remained the same as for the probe.

Specimen imaging

A 1-cm^3 specimen of outer human cerebral cortex with metastatic intracortical melanoma was obtained within 24 hours postmortem and stored in 0.9% saline. This melanoma tumor was chosen for this feasibility study because of its small (<1 mm) size and its location near the surface of the cortex. Two-dimensional imaging was performed across four metastatic lesions using the handheld surgical probe. The 1-cm^2 cortical surface area was scanned for cerebral arteries and veins. Multiple cross-sectional images were acquired along one cerebral artery. The position of the imaging beam on the cortical surface was visualized via the coincident visible aiming beam. Images (3 × 3 mm, 300 × 400 pixels) were each acquired in 30 seconds and were used for comparison with the corresponding histological findings. The handheld probe in the sample arm was then replaced with the microscope objective (*Fig. 1B*), and the tissue specimen was placed on the translational stages for three-dimensional imaging. Twenty-four cross-sectional images were acquired at 50-μm spacing to produce the three-dimensional data set. After image acquisition, the tissue was fixed in buffered formalin and underwent standard histological processing. Five-micrometer sections were stained with hematoxylin and eosin, and digital images were acquired using light microscopy.

Acquired optical coherence tomographic images and three-dimensional projections were processed using NIH Image 1.60 (National Institutes of Health, Bethesda, MD) on a Power Macintosh 9500/200 (Apple Computer, Cupertino, CA). The logarithm of the optical backscatter intensity data was displayed in two- and three-dimensional false-color images and projections. The images were threshold-segmented to reveal tumor regions of increased optical backscatter. The original images were overlaid with thresholded regions to visualize regions of tumor against surrounding cortex. Single axial reflectance profiles through normal cortex and tumor were analyzed for changes in optical properties. Linear curve fitting using the method of least squares was performed on the reflectance profiles using DeltaGraph Pro 3.5 (Delta Point, Inc., Monterey, CA). Tumor margins were determined from relative changes in optical backscatter.

RESULTS

High-resolution cross-sectional OCT of a human intracortical melanoma tumor is demonstrated in *Figure 2*. The optical coherence tomographic images in *Figure 2*, *A* and *B*, were acquired through the tumor, as indicated by the lines on the digital *en face* view of the cortex (*Fig. 2G*). These original images were threshold-segmented to identify regions of high backscatter within the tumor. The original images were then overlaid with the thresholded data and are shown in *Figure 2*, *C* and *D*. The optical coherence tomographic images show increased optical backscattering in the region of the larger tumor (*Fig. 2, white arrows*). Smaller tumor lesions also appear within the image (*Fig. 2, red arrows*). A shadowing effect is observed below each tumor because of the increased optical backscatter and the subsequent loss of optical power penetrating beneath the tumor. In *Figure 2*, *A* and *C*, the boundary of the tumor can be identified. In *Figure 2*, *B* and *D*, the tumor is identified below the surface of normal cortex. The histological findings presented in *Figure 2*, *E* and *F*, confirm the presence and relative size of the tumor. The digital image shown in *Figure 2G* illustrates the characteristic of this partic-

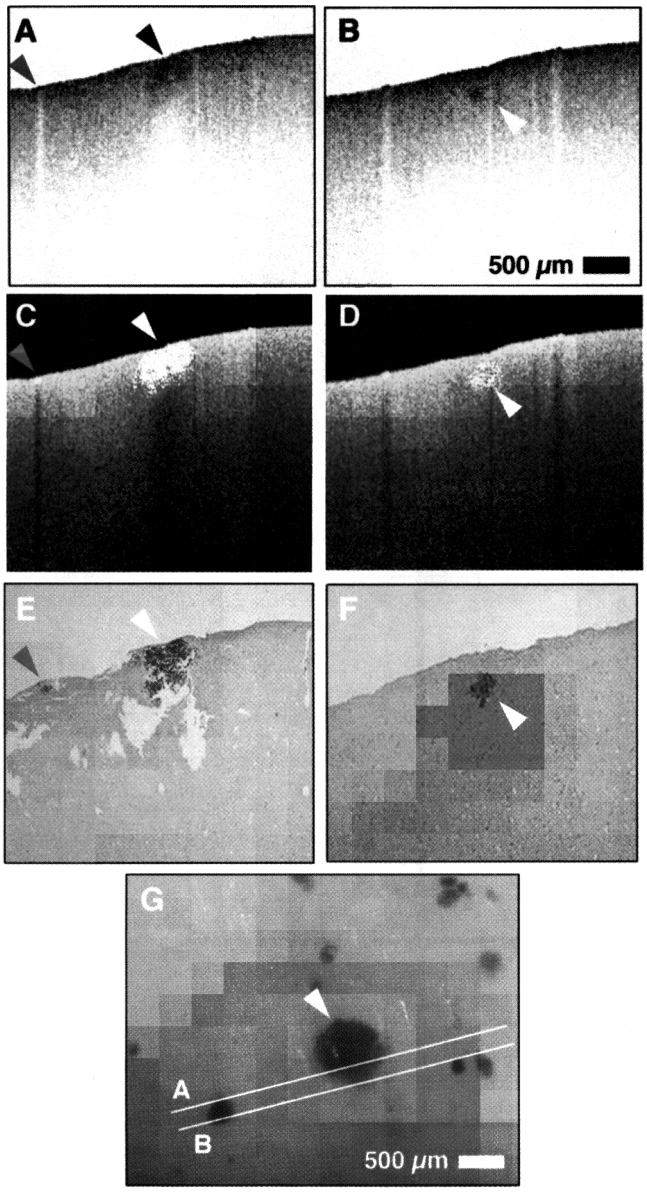

FIGURE 2. Optical coherence tomographic images and corresponding histological findings of metastatic intracortical melanoma. Unsegmented (*A* and *B*) and threshold-segmented (*C* and *D*) images illustrating tumor (*white arrow*) in cross-section. OCT permits differentiation of normal and pathological brain tissue based on changes in optical backscatter. A second, smaller region of tumor is readily identified (*red arrow*) by the shadowing effect below highly backscattering structures. *E* and *F*, corresponding histological findings showing excellent correlation with both tumor regions. *G*, digital *en face* image of tumor (*arrow*) with multiple adjacent metastases. The images in *Panels A* and *B* were acquired along the *indicated lines* shown in *Panel G*.

ular metastatic melanoma. Multiple small (<500 μm) metastases are shown surrounding the larger lesion. It is likely that the primary tumor had seeded a large number of tumor cells, which widely distributed across the gray matter of the cortex.

The location of the lower tumor margin and a quantitative assessment of the optical backscattering changes between tumor and normal cortex were obtained from single axial (depth) reflectance profiles. These are plotted in *Figure 3*. The air-tissue interfaces for the normal and tumor regions were aligned for comparison of reflectance changes with increasing depth. The plot of the normal cortex shows a uniformly attenuated reflectance with increasing depth into the cortex. A line with a slope of −0.30 dB/μm (R^2 = 0.97) was fitted to the plot of the logarithm of the optical backscatter intensity versus depth. The unit dB refers to decibels of attenuation defined as 10 log ($Power_{out}/Power_{in}$). At these wavelengths, attenuation is largely caused by scattering. Hence, the slope indicates the degree of scattering from the tissue. Using the same laser power, detection sensitivity, and beam focusing optics, an axial reflectance profile was acquired through the center of the tumor. There was an increase in optical backscatter from the surface. This reflectance profile consists of two distinct regions. Lines were fitted for each of these regions, and slopes were determined. The initial slope of −0.52 dB/μm (R^2 = 0.90) was approximately 1.7 times as steep as that for normal cortical tissue. Hence, there was nearly a twofold relative increase in optical scattering within the tumor. The second slope of −0.28 dB/μm (R^2 = 0.72) in the tumor axial profile was within 7% of the slope for normal cortex and represented normal tissue. The maximum tumor depth of 650 μm was determined by the intersection of the two fitted lines.

The axial profiles in *Figure 3* also demonstrate the maximum image penetration depth for this tissue at these optical wavelengths and power. The axial profile acquired through the normal cortex represents the backscattered signal, which attenuates exponentially (linearly on the logarithmic vertical axis) with increasing depth. At depths of 1.8 to 2.0 mm, the

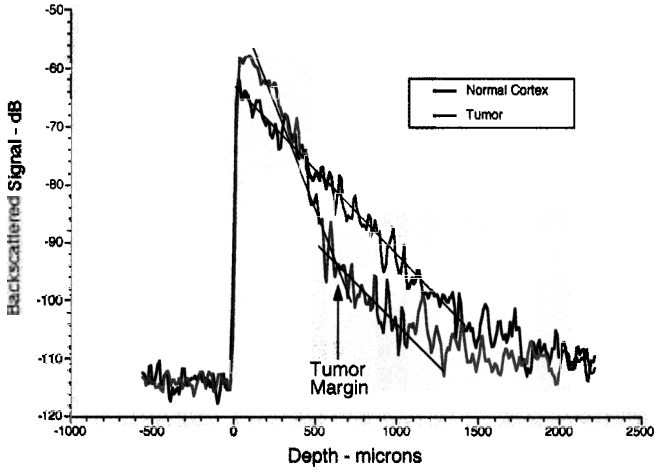

FIGURE 3. Axial reflectance plots through tumor and normal cortex. The presence of tumor results in increased optical backscatter at the surface and a higher scattering coefficient (steeper slope), as compared with normal cortex. Maximum tumor depth at 650 μm (*arrow*) is determined by changes in the slope of the axial reflectance profile. This demonstrates the use of OCT for tumor margin identification.

backscattered signal is lost in the background noise. Therefore, for the optical parameters (sensitivity of −110 dB) and tissue used in this study, ~1.8 mm is the maximum depth at which optical changes in backscatter can be detected.

Three-dimensional subsurface visualization of the intracortical melanoma and its margins is demonstrated by the projections shown in *Figure 4*. The three-dimensional data set was rotated in the horizontal and vertical planes to view the tumor at arbitrary angles. Rotation direction is indicated with respect to the superior-inferior and medial-lateral axes. Four viewing angles are shown in *Figure 4*. The two vertically rotated projections (*Fig. 4, C* and *D*) show the lower boundary of the tumor, with regions that penetrate deeper into normal cortex (*Fig. 4D, arrows*). These regions of tumor can be further visualized by sectioning the three-dimensional data set at planes parallel to the cortical surface. This orientation plane would be representative of the *en face* view of the cortical surface or, in the case of surgical removal, the resection plane as the tumor is progressively removed. The *top image* in *Figure 5* illustrates the section plane orientation through the tumor. Sections 100 to 1200 μm below the cortical surface are shown in *Figure 5*. The tumor distribution, which appears white, is shown at varying depths. The section at 1100-μm depth indicates a small region of tumor (*arrow*), which has penetrated beyond the central lesion. The color-scale transition of normal cortex from yellow (at 100 μm) to orange (at 1200 μm) is a result of signal attenuation with increasing depth. The dark region shown most prominently at 1200-μm depth is the result of shadowing from the tumor above.

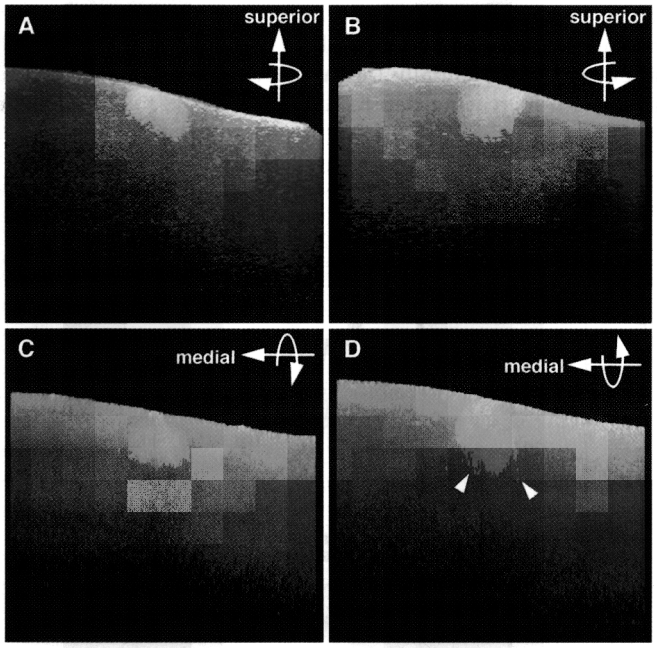

FIGURE 4. Three-dimensional projections of brain tumor. These horizontally (*A* and *B*) and vertically (*C* and *D*) rotated projections can be used to view the tumor from arbitrary angles for assessment before resection. Rotation direction is indicated with respect to the superior-inferior and medial-lateral axes. In *Panel D*, regions of the tumor (*arrows*) appear to project deeper within the surrounding cortex.

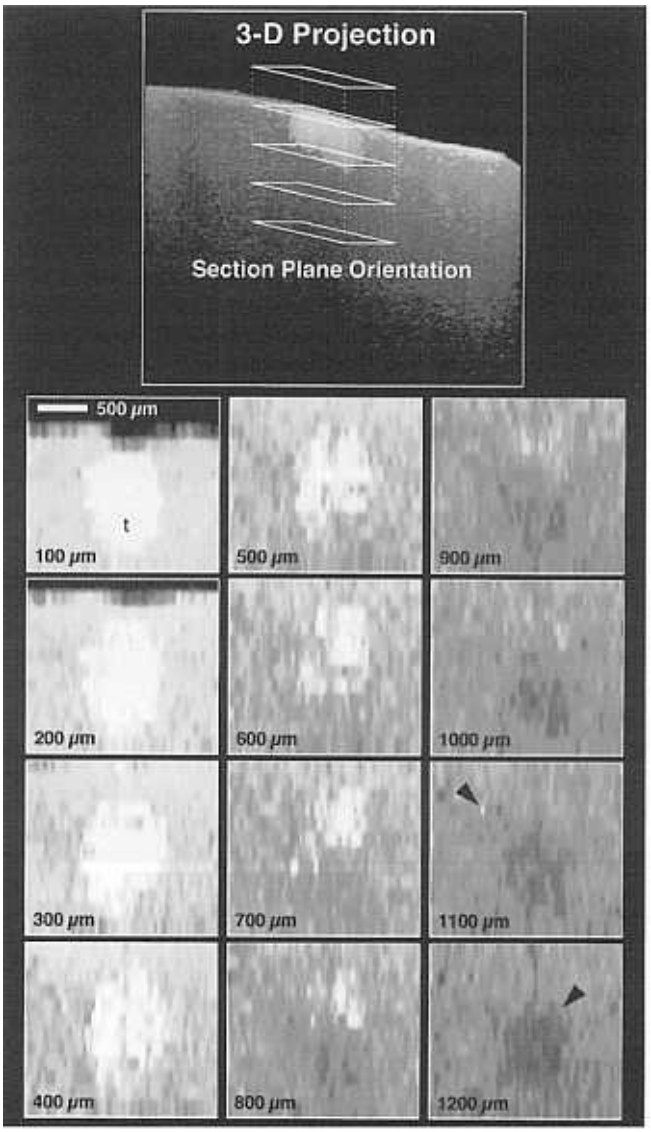

FIGURE 5. Computer sectioning of three-dimensional (*3-D*) data set at arbitrary planes. The *top image* illustrates the orientation of the planes that were sectioned parallel to the cortical surface. Sections of the tumor (*t*) at increasing depths (100–1200 μm) are shown. A small region of tumor that has penetrated below the central lesion is indicated by the *arrow* at a depth of 1100 μm. The dark region (*arrow*) shown most prominently at 1200-μm depth represents shadowing from the tumor above.

The potential of OCT for identifying subsurface vascular structures was evaluated by imaging cerebral arteries in cross-section. An optical coherence tomographic image and the corresponding histological findings are shown in *Figure 6*. The lumen of the cerebral artery is patent and clearly shown in the optical coherence tomographic image. Individual arterial layers corresponding to the intima and media can also be identified.

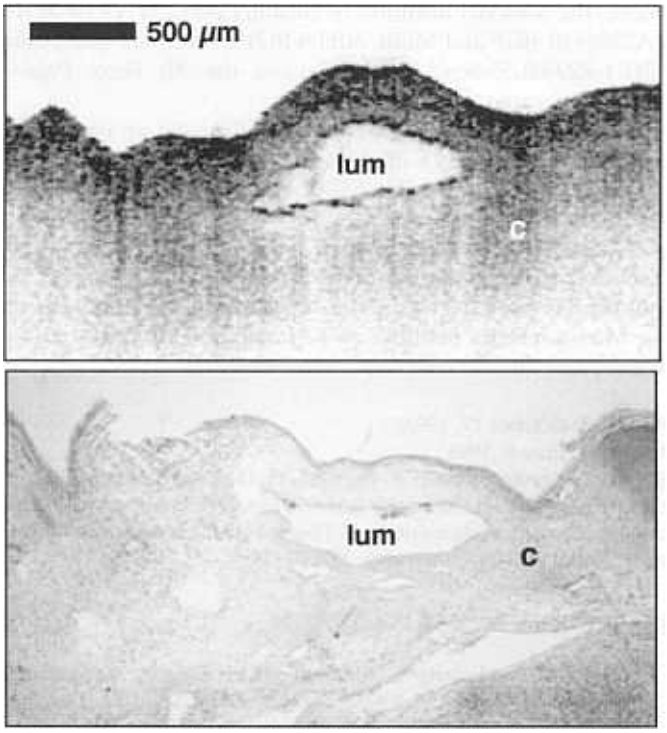

FIGURE 6. Optical coherence tomographic image and corresponding histological findings of a cerebral artery. A patent lumen is observed. The intima and media can be identified based on the higher and lower backscattering intensity, respectively. *lum*, artery lumen; *c*, normal cortex.

The intima appears as a thin, higher backscattering region surrounding the lumen of the artery. The less-backscattering media is noticeably thicker. The cerebral artery is surrounded by normal, relatively homogeneous cortex. The morphological findings observed in the optical coherence tomographic image correlate well with the corresponding histological findings. Light microscopy of this histological specimen confirms the arterial morphological findings.

DISCUSSION

In this article, we demonstrate micrometer-scale, optical coherence tomographic imaging of cadaveric human intracortical melanoma. The optical coherence tomographic images shown in *Figure 2* that were acquired with the probe show excellent correlation with the corresponding histological findings, despite the histological sectioning artifact that can be seen in *Figure 2E*. This artifact was likely caused by the different mechanical tissue properties between normal cortex and tumor, which resulted in different tensions across the microtome blade. The tumor shows increased optical backscattering compared with normal cortex. This is demonstrated quantitatively in *Figure 3*, which compares axial reflectance profiles through each tissue type.

OCT relies on the inherent contrast within tissue rather than the addition of exogenous dyes. Contrast within images is generated by variations in optical scattering, absorption, and the optical index of refraction from cellular and subcellular tissue constituents. Therefore, contrast is expected between tumors with higher concentrations of subcellular organelles (i.e., nuclei and mitochondria) and normal cortical tissue with loose supportive tissue in the gray matter (9). An intracortical melanoma was imaged for this feasibility study because it represented a small (<1 mm) focal lesion within the imaging penetration depth of this technique. The melanin within the melanoma enabled localization with the eye to position the OCT imaging beam. However, it is important to note that tissue contrast observed with the eye at visible wavelengths of light (500–700 nm) does not imply contrast at the near-infrared (1300 nm) wavelengths used in OCT. Melanin, which has a high index of refraction (n = 1.7), compared with the index for most tissue (n = 1.35), contributed to the contrast within the optical coherence tomographic images (29) but was not the only source of contrast. A previous OCT study of surgically relevant tissue found sufficient contrast between human white and grey matter, suggesting that these differences alone permit differentiation of tissue types (5). Future studies will examine other tumor morphological findings that do not contain melanin, such as astrocytomas and glioblastomas, to determine their imaging properties.

The OCT imaging depth of penetration is dependent on the optical scattering and absorption properties of the tissue as well as OCT system parameters. The longer near-infrared 1300-nm wavelength used for imaging is scattered and absorbed less than visible wavelengths. Hence, structure can be imaged at depths greater than what the eye can observe. Incident optical power and scanning speed contribute to imaging penetration. Higher powers improve imaging depth but are constrained by safety limits to prevent thermal damage to the tissue. Imaging penetration is reduced at faster scanning speeds without subsequent increase in incident power to maintain the signal-to-noise ratio. The 1.8-mm imaging depth is quantitatively shown in *Figure 3*. Although this appears somewhat limiting, particularly for larger tumors, imaging can be continuously performed ahead of the resection plane in search of the tumor margin or vulnerable structures, such as the microvasculature. *Figure 6* demonstrates OCT of a cerebral artery located below the cortical surface. Full thickness imaging of the lumen is obtained. The presence of highly scattering structures reduces the optical power available at greater depths and produces a shadowing effect. This was observed below the tumor in *Figure 5*. The presence of blood in the surgical site has a similar effect because of the large numbers of scatterers (red blood cells). The use of saline to flush the imaging site would reduce this effect.

Two-dimensional cross-sectional images of normal cortex and intracortical melanoma (*Fig. 2*) were acquired using a handheld surgical probe. The fiberoptic-based OCT instrument and probe rely on the well-established technology of the communications industry and are therefore reliable and robust. The use of optical fibers permits compact and portable instrument designs, as shown in *Figure 1A* with the handheld surgical probe. Because of the small design, implementation in the surgical field is less obtrusive, particularly because the remainder of the OCT instrument can be located elsewhere in

the room. Fiberoptic-based OCT may also be integrated with scalpels and forceps rather than introducing another instrument into the field. In the future, the probe will be used for in vivo intraoperative imaging. The noncontact nature of light permits forward-directed imaging before tissue incisions. High-power laser radiation may be coupled into the probe to allow simultaneous OCT with focused interstitial laser therapy and ablation (19). The current surgical probe design uses a single piezoelectric cantilever for transversely scanning the imaging beam and is therefore limited to two-dimensional scanning.

Three-dimensional imaging was performed using an OCT imaging microscope. Three-dimensional OCT permits multiangle visualization of the tumor and its extent, as shown in *Figure 4*. Although axis orientation and direction of rotation are provided, three-dimensional information is best obtained by observing rotation in real time. Planning for surgical resection may be improved by the acquisition of three-dimensional data sets intraoperatively. The rapid acquisition of three-dimensional volumes permits computer-based sectioning of the data sets at arbitrary planes, as demonstrated in *Figure 5*. In this example, planes sectioned parallel to the cortical surface provided visualization of tumor distribution, as would be encountered at increasing depths during tumor resection.

Future studies will focus on increasing the data acquisition rate and increasing resolution. Acquisition rates as high as eight frames per second have been achieved using the probe with a high-speed OCT system (27). However, mechanical resonances in the cantilever produced artifacts within the images. Scanning may be accomplished using small galvanometers, which would eliminate image artifacts and permit both two- and three-dimensional scanning at high acquisition rates over large cortical surface areas without having to physically move the probe. In *Figure 1B*, translation stages were used to perform three-dimensional scanning under a fixed imaging beam. This permitted precise image registration during acquisition rather than having to process and register images at a later time. The resolutions achieved in this study were as high as 16 μm, higher than with any current ultrasonographic, computed tomographic, or magnetic resonance intraoperative imaging technique. This allowed the tumor/cortex interface and the extent of tumor below the surface to be defined with high resolution. Resolutions as high as 2 to 3 μm have been achieved using solid-state ultrafast laser sources (4, 8) and may further improve the ability to localize the tumor margin.

In summary, this study investigated the feasibility of OCT as a new high-resolution optical imaging technology for neurosurgical imaging. OCT offers two- and three-dimensional imaging performance not achievable with current imaging modalities and may contribute significantly toward intraoperative neurosurgical imaging.

ACKNOWLEDGMENTS

We gratefully acknowledge Drs. Brett Bouma and Guillermo Tearney for helpful discussions and assistance. This research was supported in part by grants from the Office of Naval Research, Medical Free Electron Laser Program, Grant N00014-97-1-1066, the National Institutes of Health, Contracts NIH-9-RO1-CA75289-01 (JGF and MEB), NIH-9-RO1-EY11289-12 (JGF), and NIH-1-R29-HL55686-01A1 (MEB), and the Air Force Palace Knight Program.

The authors (SAB, MEB, CP, and JGF) have an equity interest in the company Coherent Diagnostic Technology, LLC, which has licensed intellectual property from Massachusetts Institute of Technology, Harvard Medical School, and the Massachusetts General Hospital. This relationship has been disclosed to the individual institutions, and no conflict of interest has been deemed to exist regarding the standards of the Massachusetts Institute of Technology, Harvard Medical School, and Massachusetts General Hospital.

Received, October 17, 1997.
Accepted, June 8, 1998.
Reprint requests: Stephen A. Boppart, Ph.D., Department of Electrical Engineering and Computer Science, Research Laboratory of Electronics, Massachusetts Institute of Technology, 77 Massachusetts Avenue, Room 36-345, Cambridge, MA 02139.

REFERENCES

1. Black PMcL, Moriarty T, Alexander E III, Stieg P, Woodard EJ, Gleason PL, Martin CH, Kikinis R, Schwartz RB, Jolesz FA: Development and implementation of intraoperative magnetic resonance imaging and its neurosurgical applications. **Neurosurgery** 41:831–845, 1997.
2. Boppart SA, Bouma BE, Brezinski ME, Tearney GJ, Fujimoto JG: Imaging developing neural morphology using optical coherence tomography. **J Neurosci Methods** 70:65–72, 1996.
3. Boppart SA, Bouma BE, Pitris C, Tearney GJ, Brezinski ME, Fujimoto JG: Forward-imaging instruments for optical coherence tomography. **Opt Lett** 22:1618–1620, 1997.
4. Bouma BE, Tearney GJ, Bilinsky IP, Golubovic B, Fujimoto JG: Self-phase modulated Kerr-lens modelocked Cr:forsterite laser source for optical coherence tomography. **Opt Lett** 21:1839–1841, 1996.
5. Brezinski ME, Tearney GJ, Boppart SA, Swanson EA, Southern JF, Fujimoto JG: Optical biopsy with optical coherence tomography: Feasibility for surgical diagnostics. **J Surg Res** 71:32–40, 1997.
6. Brezinski ME, Tearney GJ, Bouma BE, Izatt JA, Hee MR, Swanson EA, Southern JF, Fujimoto JG: Optical coherence tomography for optical biopsy: Properties and demonstration of vascular pathology. **Circulation** 93:1206–1213, 1996.
7. Chandler WF, Knake JE, McGillicuddy JE, Lillehei KO, Silver TM: Intraoperative use of real-time ultrasonography in neurosurgery. **J Neurosurg** 57:157–163, 1982.
8. Clivaz X, Marquis-Weible F, Salathe RP: Optical low coherence reflectometry with 1.9 μm spatial resolution. **Electronics Lett** 28:1553–1555, 1992.
9. Dunn A, Richards-Kortum R: Three-dimensional computation of light scattering from cells. **IEEE J Selected Topics in Quant Elec** 2:898–905, 1997.
10. Enzmann DR, Wheat R, Marshall WH, Bird R, Murphy-Irwin K, Karbon K, Hanbery J, Silverberg GD, Britt RH, Shuer L: Tumors of the central nervous system studied by computed tomography and ultrasound. **Radiology** 154:393–399, 1985.
11. Fujimoto JG, Brezinski ME, Tearney GJ, Boppart SA, Bouma BE, Hee MR, Southern JF, Swanson EA: Optical biopsy and imaging using optical coherence tomography. **Nat Med** 1:970–972, 1995.
12. Gooding GAW, Boggan JE, Weinstein PR: Characterization of intracranial neoplasms by CT and intraoperative sonography. **AJNR Am J Neuroradiol** 5:517–520, 1984.

13. Grimson WEL, Ettinger GJ, White SJ, Lozano-Perez T, Wells WM III, Kikinis R: An automatic registration method for frameless stereotaxy, image-guided surgery, and enhanced reality visualization. **IEEE Trans Med Imaging** 15:129, 1996.
14. Haglund MM, Hochman DW, Spence AM, Berger MS: Enhanced optical imaging of rat gliomas and tumor margins. **Neurosurgery** 35:930–941, 1994.
15. Hansen DA, Spence AM, Carksi T, Berger MS: Indocyanine green (ICG) staining and demarcation of tumor margins in a rat glioma model. **Surg Neurol** 40:451–456, 1993.
16. Hee MR, Izatt JA, Swanson EA, Huang D, Schuman JS, Lin CP, Puliafito CA, Fujimoto JG: Optical coherence tomography of the human retina. **Arch Ophthalmol** 113:325–332, 1995.
17. Huang D, Swanson EA, Lin CP, Schuman JS, Stinson WG, Chang W, Hee MR, Flotte T, Gregory K, Puliafito CA, Fujimoto JG: Optical coherence tomography. **Science** 254:1178–1181, 1991.
18. Jeannesson P, Manfait M, Jardillier JC: A technique for laser Raman spectroscopic studies of isolated cell populations. **Anal Biochem** 129:305–309, 1983.
19. Kaye AH, Morstyn G, Apuzzo MLJ: Photoradiation therapy and its potential in the management of neurological tumors. **J Neurosurg** 69:1–14, 1988.
20. Mizuno A, Hayashi T, Tashibu K, Maraishi S, Kawauchi K, Ozaki Y: Near-infrared FT-Raman spectra of the rat brain tissues. **Neurosci Lett** 141:47–52, 1992.
21. Poon WS, Schomacker KT, Deutsch TF, Martuza RL: Laser-induced fluorescence: Experimental intraoperative delineation of tumor resection margins. **J Neurosurg** 76:679–686, 1992.
22. Puliafito CA, Hee MR, Lin CP, Reichel E, Schuman JS, Duker JS, Izatt JA, Swanson EA, Fujimoto JG: Imaging of macular diseases with optical coherence tomography. **Ophthalmology** 120:217–229, 1995.
23. Schmitt JM, Yadlowsky M, Bonner RF: Subsurface imaging of living skin with optical coherence microscopy. **Dermatology** 191:93–98, 1995.
24. Scholz M, Deli M, Wildforster U, Wentz K, Recknagel A, Preuschoft H, Harders A: MRI-guided endoscopy in the brain: A feasibility study. **Minim Invasive Neurosurg** 2:33–37, 1996.
25. Taphoorn MJ, Heimans JJ, Kaiser MC, de Slegte RG, Crezee FC, Valk J: Imaging of brain metastases: Comparison of computerized tomography (CT) and magnetic resonance imaging (MRI). **Neuroradiology** 31:391–395, 1989.
26. Tearney GJ, Boppart SA, Bouma BE, Brezinski ME, Weissman NJ, Southern JF, Fujimoto JG: Scanning single-mode fiber optic catheter-endoscope for optical coherence tomography. **Opt Lett** 21:543–545, 1996.
27. Tearney GJ, Bouma BE, Boppart SA, Golubovic B, Swanson EA, Fujimoto JG: Rapid acquisition of in vivo biological images by use of optical coherence tomography. **Opt Lett** 21:1408–1410, 1996.
28. Tearney GJ, Brezinski ME, Bouma BE, Boppart SA, Pitris C, Southern JF, Fujimoto JG: In vivo endoscopic optical biopsy with optical coherence tomography. **Science** 276:2037–2039, 1997..
29. Vitkin I, Woolsey J, Wilson B, Anderson R: Optical and thermal characterization of natural (sepia oficinalis) melanin. **Photochem Photobiol** 59:455–462, 1994.

COMMENTS

Boppart et al. present a carefully performed and well-discussed experiment wherein they successfully used optical coherence tomography (OCT) for in vitro imaging of cadaveric human cortical tissue with metastatic melanoma deposits. Fujimoto and his colleagues at the Massachusetts Institute of Technology are recognized authorities in this field. This technique has potential clinical significance and is of interest to those neurosurgeons involved in neuro-oncology and the integration of real-time imaging into interactive image-guided neurosurgical tumor resections.

It must be noted that the optical properties of cadaveric specimens may differ from those encountered in living tissue because of desiccation, the absence of blood flow, the lack of movement, and the consequences of cellular death. The authors' choice of a melanoma tumor as their test case for the technique of OCT is also of note. Although I fully recognize the benefits of choosing a heavily pigmented and highly vascular tumor for a preliminary study, the reader must remain skeptical of what the results for this technique will be in other, more commonly encountered, brain tumors.

Nevertheless, the authors introduce the successful use of OCT for imaging a human brain tumor. Incorporating this technique into clinical practice will be potentially significant in selected cases of neuro-oncological resections.

Robert J. Maciunas
Rochester, New York

Modern imaging has revolutionized the diagnosis and treatment of brain tumors. In this report by Boppart et al., a new technique is described, which seems to be capable of generating images of brain tumor on a micrometer scale. Although, the potential of this method is intriguing, further experimentation is necessary. In particular, considering the possibility of a unique optical signature, the author's choice of melanoma as an experimental model may be serendipitous. Meanwhile, it is at present completely unclear how such technology might be integrated into a useful surgical device.

John R. Adler, Jr.
Stanford, California

This article describes an intriguing new intraoperative imaging tool, OCT, and illustrates its application with a cadaveric specimen of melanoma metastatic to superficial cortex. Its contribution is primarily introduction to the clinical neurosurgical community of a currently developing technology.

The application described with the particular melanoma specimen is constrained; the tumor is very superficial, small, discrete, and optically distinct from normal brain (at a broad range of wavelengths). These features appear well-suited for demonstration of feasibility, but the modality's practical applicability with more typical intracranial pathological abnormalities may prove less convincing. The maximum depth of detection described, 1.8 mm, is limiting. Conversely, the modality's particular strength of resolution on the order of micrometers is also not necessarily well matched to the proposed application. The biological nature of the disease precludes full use of such a capability; the character of the tumor boundary requires that surgical resection strategies operate at a much larger scale. Although the application described in this report has problems, it is not at all unlikely that other, very different applications, such as functional imaging or small vessel detection, may prove particularly exciting and useful.

David W. Roberts
Lebanon, New Hampshire